Theory of Néel and Valence-Bond Solid Phases on the Kagome Lattice of Zn Paratacamite

Michael J. Lawler,[1] Lars Fritz,[2] Yong Baek Kim,[1] and Subir Sachdev[2]

[1]*Department of Physics, University of Toronto, Toronto, Ontario M5S 1A7, Canada*
[2]*Department of Physics, Harvard University, Cambridge, Massachusetts 02138, USA*

(Received 9 October 2007; revised manuscript received 30 January 2008; published 5 May 2008)

Recently, neutron scattering data on powder samples of Zn paratacamite, $Zn_xCu_{4-x}(OH)_6Cl_2$, with small Zn concentration has been interpreted as evidence for valence-bond solid and Néel ordering [S.-H. Lee *et al.*, Nat. Mater. **6**, 853 (2007)]. We study the classical and quantum Heisenberg models on the distorted kagome lattice appropriate for Zn paratacamite at low Zn doping. Our theory naturally leads to the emergence of the valence-bond solid and collinear magnetic order at zero temperature. Implications of our results to the existing experiments are discussed. We also suggest future inelastic neutron and x-ray scattering experiments that can test our predictions.

DOI: 10.1103/PhysRevLett.100.187201 PACS numbers: 75.10.Jm, 75.50.Ee

Introduction.—The hallmark of frustrated magnets is the existence of macroscopically degenerate classical ground states. It is believed that quantum fluctuations about such a highly degenerate manifold may lead to unexpected quantum ground states. Proposals for emergent quantum phases include various quantum spin liquid and valence-bond solid (VBS) phases and there has been tremendous progress in a theoretical understanding of these phases during the last decade [1]. On the experimental front, ideal materials with spin-1/2 moments (without orbital degeneracy) on frustrated lattices have just become available, providing great opportunities for testing old and new theoretical proposals [2–5].

One of the prime examples is a series of recent experiments [5–10] on Zn paratacamite, $Zn_xCu_{4-x}(OH)_6Cl_2$, where Cu^{2+} ions carry spin-1/2 moments. Most of the attention has focused on the $x = 1$ limit [5], but the present Letter will address the $x = 0$ limit [6] when no Zn is present. An important advantage of the $x = 0$ limit is the absence of stoichiometric disorder, which is a serious complication in the interpretation of experiments in the $x = 1$ limit.

At $x = 1$ (herbersmithite), the idealized structure without stoichiometric disorder, has the Cu moments residing only on the layered kagome lattices. Remarkably, in the experiment no magnetic ordering has been found down to 50 mK even though the Curie-Weiss temperature is $\Theta_{CW} = -300$ K [5,7,8]. This has raised the hope that the quantum ground state of this system may be a quantum spin liquid [11–13]. As mentioned, however, the presence of stoichiometric disorder makes the interpretation of the low temperature data a difficult task.

The situation is very different near $x = 0$, where there is no intrinsic stoichiometric disorder. The magnetic lattice of the Cu^{2+} spin-1/2 moments form stacks of alternating (distorted) kagome and triangular lattices. The lattice undergoes a structural change around $x \sim 0.33$; monoclinic (rhombohedral) structure for $x < 0.33$ ($x > 0.33$) [6,10]. As a result, the magnetic lattice for $x < 0.33$ can be described as weakly coupled [6] distorted kagome lattices (see Fig. 1 for its structure).

Our theory is motivated by a recent neutron scattering experiment on powder samples of Zn paratacamite for small x [6]. These experiments find two phase transitions at finite temperature for small x. In the low temperature phase, the neutron scattering data is consistent with collinear (or Néel) magnetic ordering while no magnetic ordering is observed in the intermediate phase. Furthermore, in both phases a heavy gapped spin-1 mode is found as well as evidence for dimerization. Finally, a weak distortion in the kagome planes is observed at this x which vanishes sharply for $x > 0.33$. Based on these results, the authors of Ref. [6] propose that at small x the intermediate phase is a VBS phase which then coexists with magnetic ordering in the low temperature phase. It should be noted that identification of the intermediate phase as VBS ordered is not consistent with the interpretation of previous

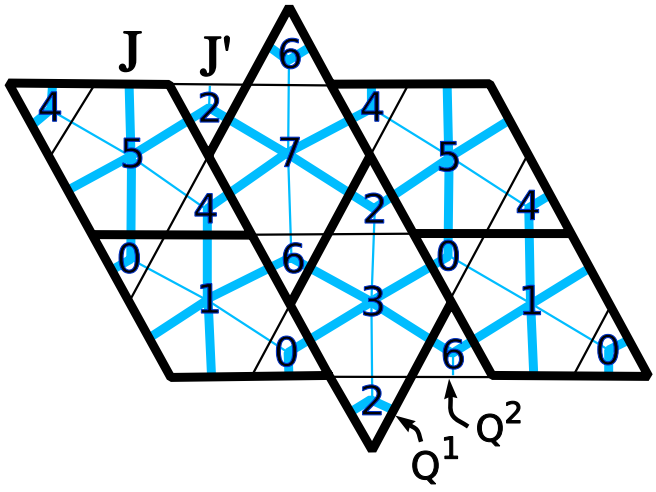

FIG. 1 (color online). Black (blue or gray) represent the distorted kagome (dual dice) lattice. The numbers, in multiples of 1/8, are the fractional offsets in the height model on the dual dice lattice which characterize the Berry's phase effects.

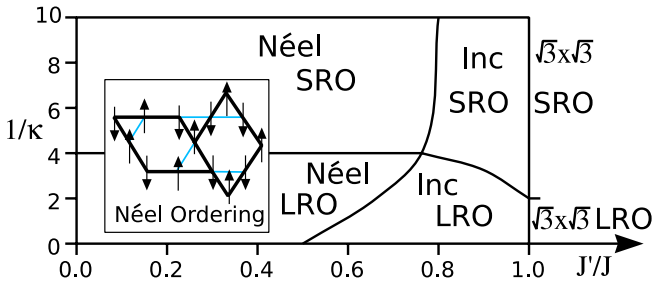

FIG. 2 (color online). The large-N Sp(N) mean field phase diagram. In the small (large) J'/J regime, the Néel (incommensurate) long-range, LRO (short-range, SRO) ordered phases arise. The inset represents the Néel ordering pattern.

μSR data [7,14] that suggest this phase is magnetically ordered. As such, further experiments, preferably on single crystals, providing more direct measurements of VBS order in the intermediate phase are necessary to reconcile these experiments. It is our aim to provide useful predictions for such studies.

In the present work, we study the antiferromagnetic Heisenberg model on the distorted kagome lattice shown in Fig. 1. We consider two inequivalent exchange interactions, $J > J'$, consistent with the distortion seen in the experiment, where J corresponds to the shorter bond length (see Fig. 1). We are mostly interested in the zero temperature ground states of this model and their connection to Zn paratacamite at $x = 0$ and possibly for small x. Using the Cu-O-Cu angles identified in the experiment, one can utilize the Goodenough-Kanamori rule to get $J'/J \approx 0.3$ [15]. In the classical Heisenberg model, we find that energetics chooses the collinear magnetically ordered state shown in Fig. 2 for $J'/J < 0.5$ and there exist highly degenerate classical ground states for $J'/J > 0.5$. The collinear state for $J'/J < 0.5$ has precisely the same magnetic order identified in the low temperature phase in Zn paratacamite for small x [6].

We then investigate the effect of quantum fluctuations and possible quantum paramagnetic phases. We use the well-documented method of the Sp(N)-generalized Heisenberg model where one can change the magnitude of "spin" to control the degree of quantum fluctuations [13,16]. The large-N mean field phase diagram of this model is presented in Fig. 2. Note that one gets the same collinear magnetically ordered state for large spin for $J'/J < 0.5$–0.8. Understanding of the nature of the quantum paramagnetic phase for small spin, however, requires careful analysis of the spin Berry's phase and quantum fluctuation effects about the saddle point solution [16,17]. We show that the resulting quantum paramagnetic state is a VBS phase depicted in Fig. 3(a). We call this the "pinwheel" VBS state. It is to be distinguished from the "columnar" VBS state [shown in Fig. 3(b)] which was suggested as a candidate valence-bond order in Ref. [6]. It can be shown [16] that the "pinwheel" state can lower the energy by the resonating moves of dimers around the "pinwheel" structures.

To provide definite predictions for the valence-bond solid phase, we compute the triplon dispersions [shown in Figs. 3(c) and 3(d)] for both of the VBS phases and suggest that inelastic neutron scattering will be able to distinguish these phases via their quite different triplon dispersions when a single crystal sample becomes available. We also suggest that an x-ray scattering experiment may clearly distinguish the two VBS ordering patterns via their different further lattice distortions induced by the ordering. The expected x-ray structure factors for both phases are shown in Fig. 4.

Classical Heisenberg model.—Possible magnetic ordering patterns in the classical Heisenberg model can be investigated by studying the $O(N)$ model in the large-N limit [18] where the 3 component spin unit vector is replaced by an N-component real-valued vector $\vec{\phi}$, with $\vec{\phi} \cdot \vec{\phi} = N$. The collinear magnetic order shown in Fig. 2, the same magnetic order observed in the experiment, is chosen for $J'/J < 0.5$ by this method. When $J'/J > 0.5$, a highly degenerate set of wave vectors have the same lowest eigenvalue and energetics alone does not determine any particular magnetic order. Thus, if magnetic ordering occurs for $J'/J > 0.5$ at finite temperatures, it should arise via a thermal order by disorder phenomenon.

Quantum Sp(N) model and mean field theory.—To investigate possible magnetically ordered and quantum paramagnetic states in the quantum antiferromagnetic Heisenberg model, it is useful to generalize the usual spin-SU(2) Heisenberg model to an Sp(N) model [16].

Let us start with the Schwinger boson representation of the spin operator $\vec{S}_r = \frac{1}{2} b^\dagger_{r\alpha} \vec{\sigma}_{\alpha,\beta} b_{r\beta}$, where $\alpha, \beta = \uparrow, \downarrow$, $\vec{\sigma}$

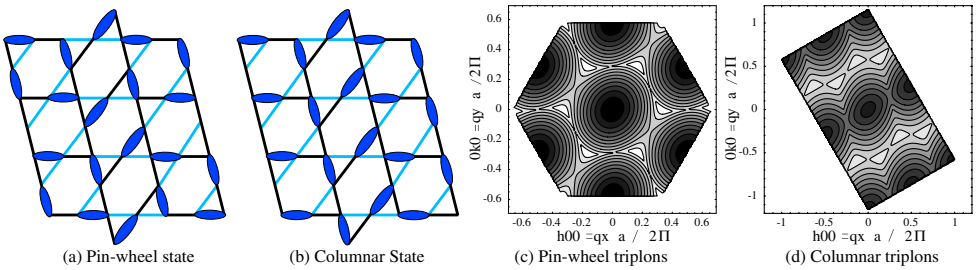

(a) Pin-wheel state (b) Columnar State (c) Pin-wheel triplons (d) Columnar triplons

FIG. 3 (color online). Pinwheel and columnar VBS states and their corresponding lowest energy triplon excitation spectra.

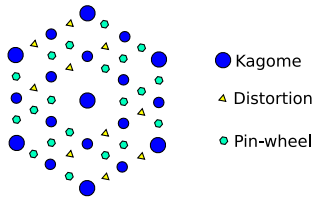

FIG. 4 (color online). X-ray structure factor: circles represent Bragg peaks of the ideal kagome lattice; triangles arise from the structural distortion shown in Fig. 1. These are the only Bragg peaks in the columnar state. In the pinwheel state, additional Bragg peaks (hexagons) appear due to further lattice distortion.

are Pauli matrices, $b_{r\alpha}$ are canonical boson operators, and a sum over repeated α indices is assumed. Note that we need to impose the constraint $n_b = b^\dagger_{r\alpha} b_{r\alpha} = 2S$ to satisfy the spin commutation relations, where S is the spin quantum number. A generalized model is then obtained by considering $2N$ bosonic fields, $b_{r\alpha}$ with $\alpha = 1, 2, \ldots, 2N$ and the constraint $n_b = b^\dagger_{r\alpha} b_{r\alpha} = 2SN$. The simplest such model with Sp(N) symmetry is

$$\mathcal{H} = \frac{1}{2}\sum_{rr'} J_{rr'} (\mathcal{J}_{\alpha\beta} b^\dagger_{r\alpha} b^\dagger_{r'\beta})(\mathcal{J}_{\gamma\delta} b_{r\gamma} b_{r'\delta}), \qquad (1)$$

where $\mathcal{J}_{\alpha\beta}$ is a $2N \times 2N$ totally antisymmetric matrix which generalizes the Pauli matrix $i\sigma_2$ from $N = 1$. When $\kappa = n_b/N = 2S$ is fixed while taking the large-N limit, the saddle point solution can be classified using both the valence-bond order parameter $Q_{rr'} = \langle \mathcal{J}_{\alpha\beta} b^\dagger_{r\alpha} b^\dagger_{r'\beta} \rangle$ and the magnetization induced by a finite condensate $x_{r\alpha} = \langle b_{r\alpha} \rangle$. The advantage of the large-N mean field theory is that we can investigate both the large-κ semiclassical limit and the small-κ extreme quantum limit on an equal footing [16].

In the distorted kagome lattice, we need two inequivalent valence-bond order parameters, $Q^1_{rr'}$ and $Q^2_{rr'}$, as depicted in Fig. 1. We also need two Lagrange multipliers for two inequivalent sites to impose the constraint $b^\dagger_{r\alpha} b_{r\alpha} = \kappa N$. These parameters need to be determined self-consistently in the large-N mean field theory. The large-N Sp(N) mean field phase diagram for the distorted kagome lattice is shown in Fig. 2. For $\kappa > \kappa_c = 0.26$, the collinear magnetically ordered state (Fig. 2) appears in the $J'/J < 0.5$–0.8 regime; this is the same magnetic order as discovered in the experiment and in the classical model. For $J'/J > 0.5$–0.8 and at large κ, the ground state acquires an incommensurate coplanar order and becomes the $\sqrt{3} \times \sqrt{3}$ state at $J' = J$ [1]. The nature of the paramagnetic state for small $\kappa < \kappa_c$, however, cannot fully be determined within the mean field theory.

Quantum fluctuations and valence-bond solid in the paramagnetic phase.—Understanding of the paramagnetic phases requires careful analysis of spin Berry's phase and quantum fluctuation effects about the mean field solution [16,17]. It is important to note that $Q^2_{rr'} = 0$ in the paramagnetic phase for small $J'/J < 0.5$–0.8. Thus this phase is adiabatically connected to the $J' = 0$ limit, corresponding to the bipartite lattice depicted by the thick lines in Fig. 1. Using $Q^1_{rr'} = Q_1 e^{iA_{rr'}}$, one can clearly see that the action in this $Q^2_{rr'} = 0$ paramagnetic phase is invariant under the U(1) gauge transformation: $b_{r\alpha} \to e^{i\theta_r} b_{r\alpha}$ ($b_{r\alpha} \to e^{-i\theta_r} b_{r\alpha}$) for r on the A sublattice (B sublattice) and $A_{rr'} \to A_{rr'} + \theta_r - \theta_{r'}$. The effective field theory of such a paramagnetic phase is given by the gapped bosonic spinons carrying ± 1 gauge charges (depending on the sublattices) coupled to a U(1) gauge field $A_{rr'}$. Since the spinons are gapped in the paramagnetic phase, integrating them out in general produces a $2 + 1$ dimensional compact U(1) lattice gauge theory captured by the simple partition function [1]

$$Z = \int \prod_{\langle ij \rangle} \frac{dA_{ij}}{2\pi} \exp\Big[\sum_p V(\mathrm{curl}_p \mathbf{A}) + i \sum_{\langle ij \rangle} \eta_{ij} A_{ij} \Big], \qquad (2)$$

where $\langle ij \rangle$ represent the nearest-neighbor sites of the space-time lattice (here we have discretized time) and $V(\Phi) = V(-\Phi) = V(\Phi + 2\pi)$ is an arbitrary periodic potential. Here p labels the plaquette of the space-time lattice and $\mathrm{curl}_p \mathbf{A} = \sum_{\langle ij \rangle \in p} \mathrm{sgn}_p(ij) A_{ij}$, where $\mathrm{sgn}_p(ij) = -\mathrm{sgn}_p(ji) = 1$ if j comes right after i when one goes around a given plaquette p and $\mathrm{sgn}_p(ij) = 0$ otherwise. Here η_{ij} is an external current determined by spin Berry's phase and it is given by $\eta_{ij} = \eta_{(rt),(r't')} = \pm \delta_{rr'} \delta_{t+1,t'}$ (for spin-1/2) depending on whether r belongs to the A or B sublattice. Thus the problem reduces to the compact U(1) gauge theory with background charges of ± 1 at the A and B sublattice [1]. As is well known, this compact U(1) gauge theory is confining and the resulting ground state would most likely be a VBS.

To find the nature of the VBS state, it is useful to construct the so-called height model on the dual lattice [1], which is equivalent to the compact U(1) gauge theory on the direct lattice. The height model can be derived using the well-documented duality transformation and written in terms of the integer-valued height fields $h_{\bar{\imath}}$ defined on the sites $\bar{\imath}$ of the dual space-time lattice [1]. In our case the dual lattice (in a given time slice) is a distorted dice lattice $\{\bar{r}\}$ as shown in Fig. 1 (blue or gray lattice). Note that the thick blue lines correspond to the dual lattice of the $J' = 0$ limit of the original distorted kagome lattice. The height model is found to have action (see the online EPAPS supplementary material [19])

$$S_h = \sum_{\langle \bar{\imath}\bar{\jmath} \rangle} \frac{g}{2} (h_{\bar{\imath}} - h_{\bar{\jmath}} + \zeta_{\bar{\imath}} - \zeta_{\bar{\jmath}})^2, \qquad (3)$$

where $\langle \bar{\imath}\bar{\jmath} \rangle$ are the thick bonds of the distorted dual space-time lattice and g a nonuniversal coupling constant. Here the constraint $h_{\bar{\imath}} = h_{\bar{\jmath}}$ must be imposed if $\bar{\imath}\bar{\jmath}$ is a thin bond and the offset variables $\zeta_{\bar{\imath}}$ are determined by the spin Berry's phase and their time independent site-dependent values $(\frac{1}{8}, \frac{6}{8}, \frac{3}{8}, 0, \frac{5}{8}, \frac{2}{8}, \frac{7}{8}, \frac{4}{8})$ on the dice lattice are shown in

Fig. 1. After solving the simple constraint, this height model can be understood using standard methods [16] and the average height fields can be determined up to an overall constant [1].

The nature of the VBS ground state can be studied by using the relation between the height fields and the VBS order parameter. It can be shown that the ''electric field'' [in the compact U(1) gauge theory] defined on the spatial dual-lattice links is related to the height fields via $e_{\bar{r}\bar{r}'} = \langle h_{\bar{r}} \rangle - \langle h_{\bar{r}'} \rangle$ [1]. The VBS order parameter defined on the direct-lattice link that intersects the spatial dual-lattice link $\langle \bar{r}\bar{r}' \rangle$ is given by the strength of $e_{\bar{r}\bar{r}'}$ [1]. The result is a ''pinwheel'' pattern shown in Fig. 3(a).

Neutron scattering: triplon dispersion.—In Ref. [6], a different VBS phase [see Fig. 3(b)]—the columnar phase—was suggested. Here we show that different triplon dispersions in the pinwheel and columnar VBS phases can be used to distinguish them if inelastic neutron scattering experiments are done on single crystals.

To compute the triplon dispersion, consider letting J be the exchange interaction between two spins within the same valence bond and λJ between two spins on different nearby valence bonds. In the decoupled $\lambda = 0$ limit, the triplon dispersion would be completely flat with energy J. When λ is finite, the triplon band disperses. Here we compute this dispersion to first order in λ. For this purpose, we apply the bond-operator formalism [20] to the valence bonds in the VBS phases where the Hilbert space can be represented via singlet and triplet states on the bonds of Fig. 3. At first order in λ, only the processes that preserve triplon number contribute, and to this order they become dispersing particles. These dispersions for the lowest band in both the pinwheel and columnar states are shown in Figs. 3(c) and 3(d). The minima in the two cases are clearly located at different positions, a feature that can be distinguished experimentally.

X-ray scattering.—Assuming a lattice contraction where valence bonds exist, the pinwheel state should break the lattice translational symmetry of the distorted kagome lattice in one of two directions, doubling the unit cell. This would lead to new peaks in the x-ray structure factor. However, the lattice translational symmetry would be intact in the columnar state, leading to no new Bragg peaks in the x-ray structure factor in addition to those associated with the distorted kagome lattice. The x-ray structure factors for the two VBS phases are shown in Fig. 4. Note that the hexagon symbols represent the new Bragg peaks in the pinwheel state. All other peaks also exist in the columnar state.

Summary and conclusion.—We have provided a theory of the zero temperature phases of an antiferromagnetic Heisenberg model on a distorted kagome lattice. The resulting VBS and Néel ordered phases are strikingly similar to those identified in the recent neutron scattering experiment on Zn paratacamite at small doping x [6]. In particular, our theory predicts that ''pinwheel'' VBS ordering [see Fig. 3(a)] can occur as a result of quantum disordering of the Néel order. We have suggested future neutron and x-ray scattering experiments that can test our predictions for this ''pinwheel'' VBS ordering. Our predictions may also be used for future resolution of the disagreement between the interpretations of the neutron scattering and μSR data in the intermediate temperature phase. Furthermore, here we focused on zero temperature ground states of a Heisenberg model so that an explanation of the coexistence of Néel and VBS ordering at finite temperature is beyond the scope of this work. However, we note that a phase transition between the two phases is likely to be first order, leaving the possibility of a coexist region in the phase diagram. The possible relation between the quantum phases on the distorted kagome lattice described here and the yet-to-be-determined quantum ground state [1,11–13,21,22] on the ideal kagome lattice is an important subject of future research.

This work was supported by NSERC, CIFAR, CRC, and No. KRF-2005-070-C00044 (M. J. L., Y. B. K.); NSF Grant No. DMR-0537077 (L. F., S. S.); Deutsche Forschungsgemeinschaft under Grant FR No. 2627/1-1 (L. F.). We thank S.-H. Lee, A. Vishwanath, and M. Hermele for helpful discussions, and acknowledge the Aspen Center for Physics.

[1] For a review on theoretical progress, see S. Sachdev, Ann. Inst. Henri Poincaré **4**, 559 (2003).
[2] Z. Hiroi *et al.*, J. Phys. Soc. Jpn. **70**, 3377 (2001).
[3] Y. Shimizu *et al.*, Phys. Rev. Lett. **91**, 107001 (2003).
[4] Y. Okamoto *et al.*, Phys. Rev. Lett. **99**, 137207 (2007).
[5] J. S. Helton *et al.*, Phys. Rev. Lett. **98**, 107204 (2007).
[6] S.-H. Lee *et al.*, Nat. Mater. **6**, 853 (2007).
[7] P. Mendels *et al.*, Phys. Rev. Lett. **98**, 077204 (2007).
[8] O. Ofer *et al.*, arXiv:cond-mat/0610540.
[9] T. Imai *et al.*, Phys. Rev. Lett. **100**, 077203 (2008).
[10] M. A. de Vries *et al.*, arXiv:0705.0654.
[11] Y. Ran *et al.*, Phys. Rev. Lett. **98**, 117205 (2007).
[12] S. Ryu, O. I. Motrunich, J. Alicea, and M. P. A. Fisher, Phys. Rev. B **75**, 184406 (2007).
[13] S. Sachdev, Phys. Rev. B **45**, 12 377 (1992).
[14] X. G. Zheng *et al.*, Phys. Rev. Lett. **95**, 057201 (2005).
[15] S.-H. Lee (private communication); in Proceedings of the KITP Conference on 'Motterials,' 2007 (unpublished).
[16] N. Read and S. Sachdev, Phys. Rev. Lett. **66**, 1773 (1991).
[17] F. D. M. Haldane, Phys. Rev. Lett. **61**, 1029 (1988).
[18] D. A. Garanin and B. Canals, Phys. Rev. B **59**, 443 (1999).
[19] See EPAPS Document No. E-PRLTAO-100-051817 for height model derivation. For more information on EPAPS, see http://www.aip.org/pubservs/epaps.html.
[20] S. Sachdev and R. N. Bhatt, Phys. Rev. B **41**, 9323 (1990).
[21] For a review, see C. Lhuillier, arXiv:cond-mat/0502464.
[22] C. Zeng and V. Elser, Phys. Rev. B **42**, 8436 (1990); J. B. Marston and C. Zeng, J. Appl. Phys. **69**, 5962 (1991); M. B. Hastings, Phys. Rev. B **63**, 014413 (2000); P. Nikolic and T. Senthil, Phys. Rev. B **68**, 214415 (2003); R. R. P. Singh and D. A. Huse, Phys. Rev. B **76**, 180407 (2007).